RESEARCH PAPER

Keyhole welding with CF-TIG (cathode focussed GTA)

M. Lohse · U. Füssel · H. Schuster · J. Friedel · M. Schnick

Abstract In this paper, the results for keyhole welding of stainless steel 1.4301 and mild steel 1.0117 with a cathode focussed gas tungsten arc process are presented. These tests were carried out in preparation for welding the root faces of Y- or double V-groove weld preparations of thick metal plates. Welded plate thicknesses range from 6 to 10 mm for stainless steels and 6 to 12 mm for mild steels. Welding speeds are in the range of 20 to 115 cm/min at currents from 400 to 800 A. Especially for stainless steel, a big range of applicable and stable process parameters could be found. The process also works fine for mild steel even though the achievable parameter range is smaller.

Keywords Cathodes · GTA welding · TIG welding · Stainless steels

1 Introduction

To weld metal plates with thicknesses up to 80 mm, Y- or double V-groove weld preparations can be used [1]. First, the root faces are welded, and consecutively, the remaining groove is filled, e.g. with submerged arc welding (SAW). Conventionally, the root faces are joined using a GMAW process with penetration depths around 3 mm. By performing the root face weld with the keyhole technique

in one pass, several benefits emerge. First, the time for welding the back pass is reduced. Second, the weld volume for the subsequent filling is reduced and so are the heat input, the filler material needed and the welding time. Finally, the deeper back pass reduces the possibility of sagging of the subsequent weld (i.e. SAW) (Fig. 1).

Commonly used processes for performing keyhole welding are laser [2, 3] and plasma welding [4, 5] due to their high energy densities [6]. But using a laser is bound to the restrictive security measures that have to be considered for the high-energy beam. Plasma welding torches in turn are restricted by their relatively large sizes [5], since the plasma nozzle for constricting the arc has to be incorporated into the torch design [7]. Thus, problems may arise in positioning the torch into the weld seam preparation.

These drawbacks may be circumvented using a gas tungsten arc (GTA) process, but the common GTA arc is not sufficiently powerful to go into a keyhole mode. One possibility for GTA-keyhole welding is presented in [8]. Good results have been achieved for several materials like austenitic steels, titanium alloys and duplex stainless steels as well as zirconium. Weldable thicknesses up to 12 mm have been found for austenitic steel. However, the process is said to be limited to materials with low thermal conductivities [9].

In [10], a new GTA torch with a highly constricted arc is presented. The design of this torch is shown in Fig. 2.

The arc constriction is achieved by using a specially designed and cooled cathode as described in [11]. Due to the cooling, the thermo-emittive behaviour of the cathode is influenced leading to a smaller area where the arc can attach to the cathode surface, thus increasing the current density and therefore the arc constriction [11]. Thanks to this unique arc property, the torch can be used to perform GTA-keyhole welding. In this paper, the torch is used to experimentally investigate whether stainless steel and mild steel can be joined in one pass using the cathode focussed tungsten inert gas (CF-TIG) process.

M. Lohse (✉) · U. Füssel · M. Schnick
Institute of Surface and Manufacturing Technology,
Dresden University of Technology, Dresden, Germany
e-mail: martin.lohse@tu-dresden.de

H. Schuster · J. Friedel · M. Schnick
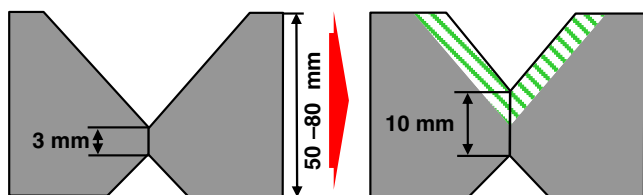Kjellberg Finsterwalde Plasma und Maschinen GmbH,
Finsterwalde, Germany

Fig. 1 Reduction of the weld cross section due to an increase of the root face size

In the first part of the paper, the experimental setup is explained. In the second part, the welding results for stainless steels are shown and an interpretation is given. The third part deals with keyhole welding of mild steel, and the first results are shown. Finally, conclusions are given.

2 Experimental setup

The experimental setup consists of a clamping unit to fix the specimen and prevent distortion due to the heat input. The CF-TIG torch is guided linearly over the specimen by an articulated robot. The weld is shielded by a pure argon shielding gas, trailing gas and back purge. For distributing the trailing gas, a custom-built trailing shield attached to the welding torch is used. The back purging is done by a custom-built distributor pipe fitted into the clamping unit (Fig. 3).

The gas flow rates were 15 L/min for the shielding gas and 20 L/min for the trailing shield and the back purge,
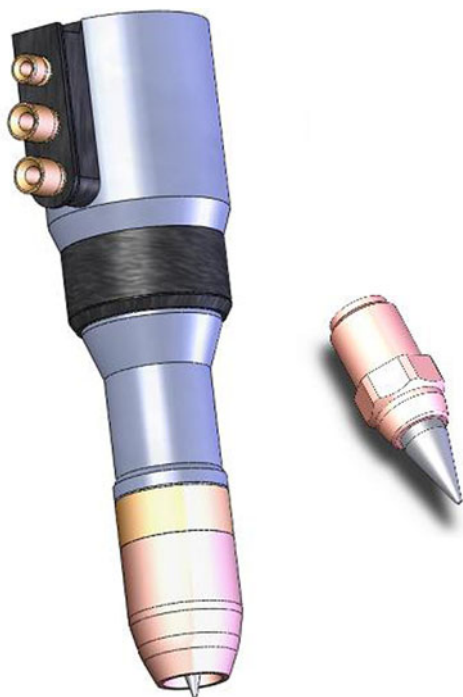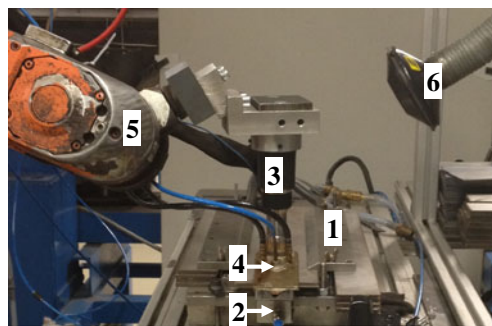

Fig. 3 Experimental setup consisting of clamping unit (*1*), forming gas distributor (*2*), CF-TIG torch (*3*), trailing gas shield (*4*), articulated robot (*5*), and fume extraction (*6*)

respectively. The tungsten cathode used was made of WLa15 and had a diameter of 6.4 mm, a conical tip with an included angle of 30° and a flat tip of radius 0.5 mm. The cathode extension from the shielding cup was 4.5 mm, and the cup diameter was 16 mm.

The specimens were plasma cut from metal blanks without any further edge preparation. Thus, the joints had a square butt configuration, and the gap between the plates was set to 0.5 mm. The plasma cut faces have a maximal roughness Rmax=6.69 μm and a total height of the roughness profile Rt=7.11 μm for the 6-mm specimens. The values for the 10-mm specimens are as follows: Rmax=6.69 μm and Rt=14.21 μm. The average groove width RSm=1.6 mm for the 6-mm specimens and RSm=1.9 mm for the 10-mm specimens.
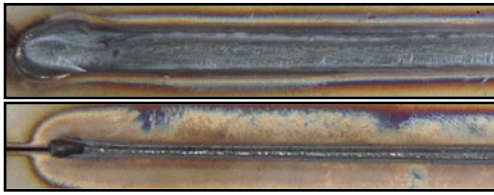
The material investigated was X5CrNi18-10 (EN 1.4301) for the stainless steel tests and S235J2G2+C (EN 1.0117) for the mild steel tests. All experiments were carried out without using filler wire.

The welding current and the welding speed were systematically varied to find appropriate welding parameters. These experiments were carried out for three different distances between the cathode tip and the workpiece surface (CWD).

3 Results for stainless steel

The gap between the plates is a parameter that normally varies throughout any common welding process. Therefore, the influence of a non-constant gap on the welding result of GTA-keyhole welding is determined first. To do so, two specimens were fitted together with a 0-mm gap on one end and a 2.6-mm gap on the other. The torch was positioned to always be in the middle of the gap at a constant cathode tip-to-workpiece surface distance of 2 mm. As can be seen in Fig. 4, the weld seam is formed evenly over the complete gap range. Even though the weld seam is significantly sagging for big gap values, there is a good root formation.

Fig. 2 Design of the cathode focussed welding torch and its cathode and shielding cup

start of weld(0 mm gap)
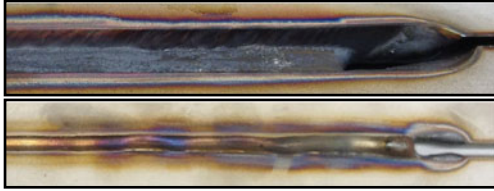

end of weld(2.6 mm gap)

Fig. 4 Appearance of weld seam for different gaps between the welded metal plates; the *upper picture* shows the weld surface, and the *lower picture* shows the weld root

Although it could be proven that the process works for a 0- to 2.6-mm gap, the result showed that a small gap, i.e. 0.5 mm, is beneficial for the keyhole formation, especially for thicker specimens. Therefore, the gap between the metal plates was always set to 0.5 mm.

3.1 6-mm-thick specimens

First, 6-mm-thick specimens were welded. A wide range of parameters could be found that were appropriate to join the plates. The CWD was set to 2 mm. Welding currents ranged from 400 to 700 A and the welding speed from 25 up to 95 cm/min, as can be seen in Fig. 5. At low welding currents, the energy density of the arc is not sufficient for the keyhole mode, so 400 A marks a lower limit of applicable welding currents. The widest parameter range could be found for 500 A which is found to be the optimal welding current for 6-mm-thick stainless steel plates. For higher welding currents, the lower achievable welding limit increases linearly from the lower welding currents, while the parameter range is reduced. However, the range of achievable welding speeds
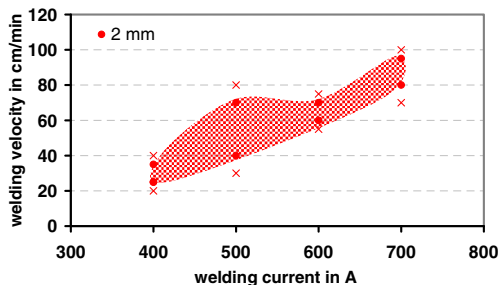

Fig. 5 Range of parameters for joining 6-mm-thick specimens with a CWD of 2 mm, *full dots* marking valid tests, *crosses* marking excessive or insufficient penetration

stays the same for 600 and 700 A, having the highest welding speeds for 700 A.

The resulting weld seam cross sections are shown in Fig. 6. The etchant used was one part aqua regia in one part distilled water and an addition of 0.02 parts "Dr. Vogels Sparbeize". All cross sections show a V-shaped fusion zone. According to [12], a heat-affected zone (HAZ) should be visible with the etchant used. However, in the pictures of the cross sections, such a zone is nearly not observable. Only for welding speeds lower than 60 cm/min can it be argued that there is a region between the molten and the base material. From this, it is assumed that the HAZ is very small due to the high welding speeds and the low thermal conductivity of the stainless steel. It can be argued that this is in good agreement with the very low distortion of the specimens that was found. Furthermore, the weld seam root is well formed, even when the metal plates show some mismatch in height. Additionally, the cross sections show no imperfections such as cracks, inclusions or lack of fusion. However, undercut and underfill occur for higher welding speeds and welding currents.

It can be seen that for low welding speeds and low welding currents, the weld seam surface has a smooth transition to the non-molten metal, and that the root of the weld is quite large. If the welding speed was reduced under the lower limit, sagging occurred.

For higher welding speeds, the pictures show a smaller root with virtually no sagging. In turn, undercuts appear on the weld seam surface especially for high welding currents. Insufficient penetration occurred for welding speeds higher than the upper limit.
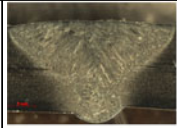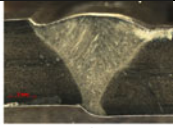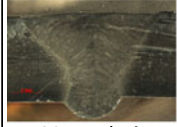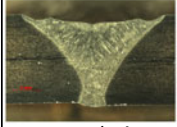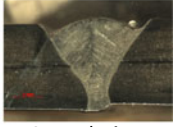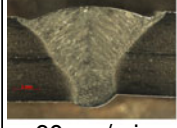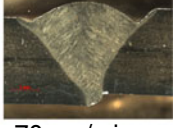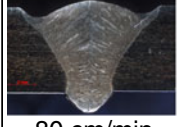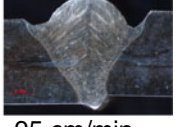

Fig. 6 Cross sections of 6-mm-thick specimens for the parameter range of Fig. 5 for a CWD of 2 mm

After successfully finding parameters to weld 6-mm stainless steel plates, the influence of the CWD was investigated and was set to 4 mm in a second test series. The parameters found are shown in Fig. 7.

In Fig. 7, the ranges of welding parameters for 2- and 4-mm CWDs are compared, and it can be deduced that the range of parameters for good welding results is approximately the same for welding currents up to 500 A. Above that, for a CWD of 4 mm, deep undercuts are more likely, and the upper limits are reduced. In Fig. 8, it can also be seen that lack of fusion occurs for the upper welding speed limit at 500 A.

Increasing the CWD showed a decrease in appropriate welding parameters, where even lack of fusion occurred. Hence, in the next test series, the CWD was set to 0.5 mm (Fig. 9).

In Fig. 9, the parameter range for a CWD of 0.5 mm is shown. The area below a welding current of 600 A is quite similar to the test series with a CWD of 2 mm. But, for a higher welding current of 700 A, a fully penetrated weld is possible up to 115 cm/min. In turn, the weld seam surface becomes irregular, showing undercuts of varying depth (Fig. 10). Still, all cross sections show no welding imperfections apart from undercut and underfill (Fig. 10).

Since a low CWD has proven to be beneficial for the welding speed as well as the weld seam quality, a test was carried out with a negative CWD, i.e. the cathode tip moves below the workpiece surface. In order to get a good comparability for different CWDs, the value was made variable over the welding length. The resulting weld seam surface is shown in Fig. 11. It can be seen in Fig. 11 that a negative CWD leads to a reduction of the width of the weld seam surface as well as to a reduction of undercut, while the root formation is virtually not influenced.

Thus, it can be said that the CF-TIG process offers a wide range of parameters to join 6-mm-thick stainless steel plates at high welding speeds and with good weld seam qualities. With suitable equipment to adjust the CWD to negative values, the weld seam quality can be enhanced further.
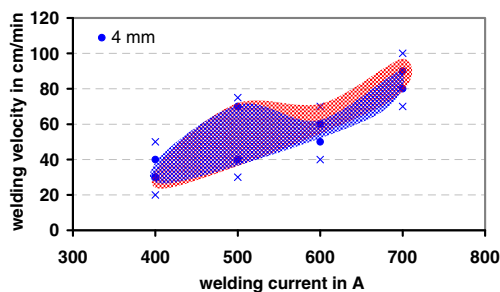

Fig. 8 Cross sections of 6-mm-thick specimens for the parameter range of Fig. 7 for a CWD of 4 mm

3.2 8-mm-thick specimens

Following the findings from the testing of 6-mm-thick specimens, a CWD of 0.5 mm is used for all tests with 8-mm-thick specimens. A negative CWD is for now omitted for the sake of experimental simplicity. In Fig. 12, the acceptable welding parameters are shown.

As expected, the applicable range of parameters for good welding results shrinks, and all welding speeds found for

Fig. 7 Range of parameters for joining 6-mm-thick specimens with a CWD of 4 mm, *full dots* marking valid tests, *crosses* marking excessive or insufficient penetration; the *red area* represents range for a CWD of 2 mm
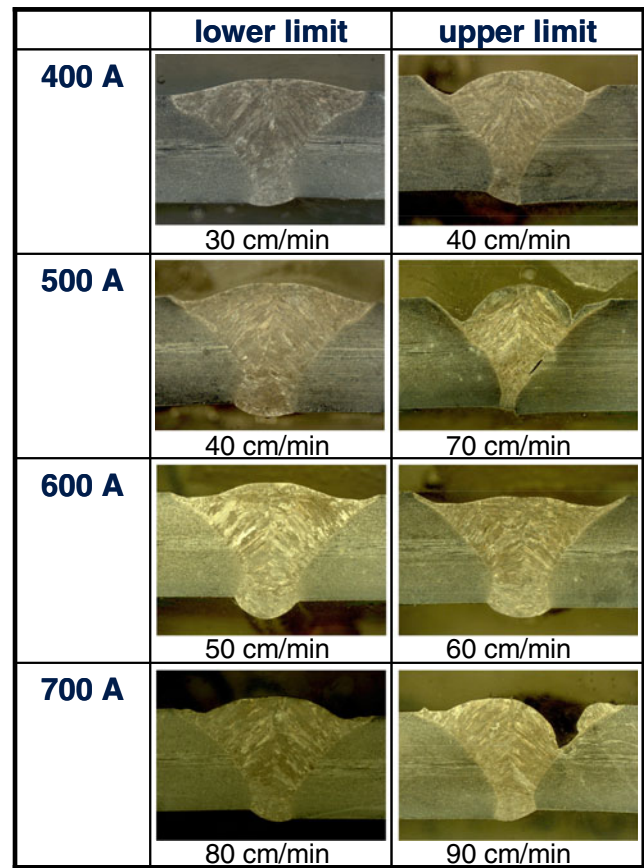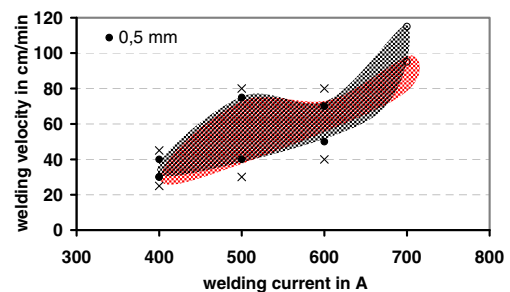

Fig. 9 Range of parameters for joining 6-mm-thick specimens with a CWD of 0.5 mm, *full dots* marking valid tests, *circles* marking tests with irregular weld seam surface, and *crosses* marking excessive or insufficient penetration; the *red area* represents range for a CWD of 2 mm
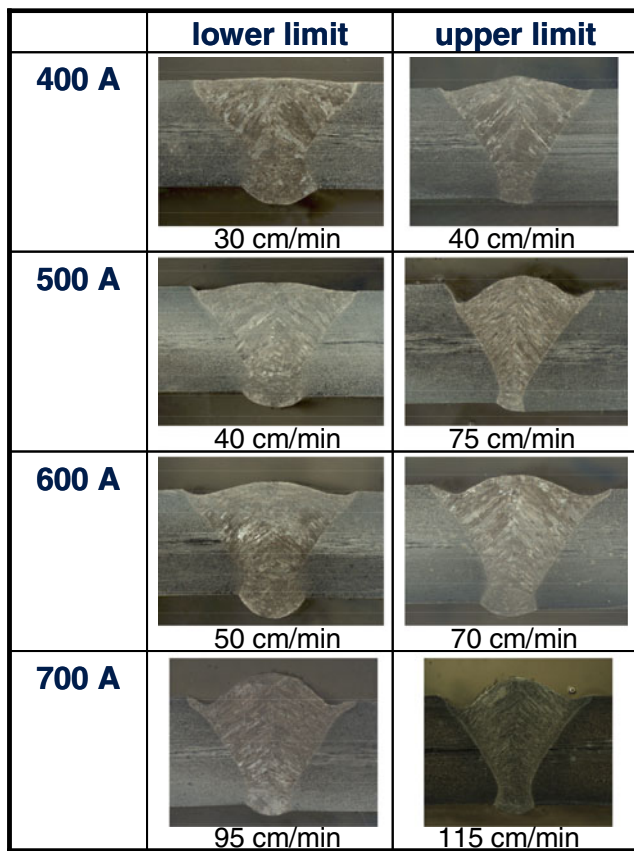
Fig. 10 Cross sections of 6-mm-thick specimens for the parameter range of Fig. 9 for a CWD of 0.5 mm

Fig. 12 Range of parameters for joining 6- and 8-mm-thick specimens with a CWD of 0.5 mm, *full symbols* marking valid tests, *empty symbols* marking tests with irregular weld seam surface

is smaller for the 6-mm specimen. Still, the bottom specimen edges are entirely molten into the weld root.

With the 8-mm-thick stainless steel tests, a smaller but stable range of parameters could be found in comparison to the 6-mm tests. The likely appearance of underfill will probably necessitate the use of filler wire.

3.3 10-mm-thick specimens

After finding that filler wire might already have to be used for 8-mm-thick specimens, only a limited number of tests were performed with 10-mm-thick stainless steel plates to prove feasibility. The results are shown in Fig. 14. Again, the cross sections show no imperfections but undercut and underfill. The described effect of underfill for 8-mm plates due to the gap in the weld preparation is of course stronger for 10-mm plates.

8 mm lie below the values for the 6-mm-thick specimens. In contrast to the results for 6 mm, the achievable welding speed limits increase linearly for the upper and the lower bound. Furthermore, a slight increase of the parameter range can be observed for increasing welding currents.

The cross sections for the 8-mm specimen show V-shaped fusion zones with no imperfections but undercut and underfill (Fig. 13). For all but one test, underfill appears, and that can be expected based on the gap used between the metal plates since this gap has to be filled with base material, so thicker plates lead to more material needed to fill the joint. Furthermore, the weld root width to weld seam surface width
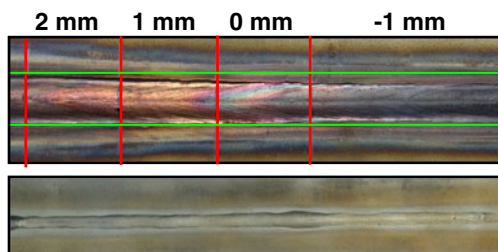

Fig. 11 Weld seam surface for different CWDs at a constant welding current of 500 A and a constant welding speed of 55 cm/min
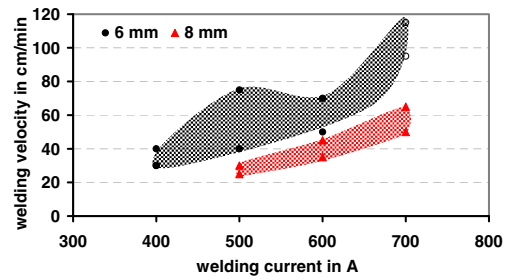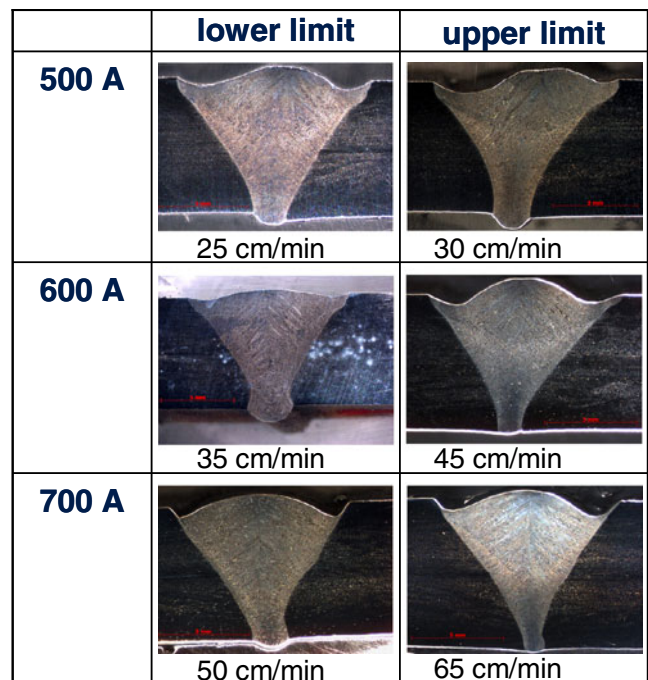

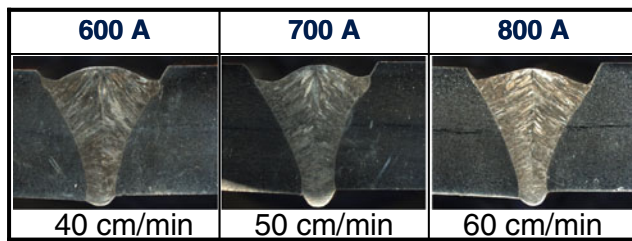Fig. 13 Cross sections of 8-mm-thick specimens for the parameter range of Fig. 12 for a CWD of 0.5 mm

Fig. 14 Cross sections of 10-mm-thick specimens for different welding currents and welding speeds with a CWD of 0.5 mm

4 Results for mild steel

4.1 6-mm-thick specimens

Following the test series for stainless steels where welding parameters for up to 10-mm-thick metal plates could be found, mild steels were investigated. The cross sections for the first parameters found are shown in Fig. 15. The etchant used was 5 % nital. For mild steels, the back purge is one of the main factors influencing the weld seam formation, since the surface tension is strongly affected by the oxygen contamination of the gas at the weld root. Oxygen leads to a decrease in surface tension resulting in a sagging weld seam. Therefore, as can be seen in Fig. 15, the welding parameter range is much more restricted compared to stainless steels.

Still, it is valid that low welding speeds and welding currents lead to smooth weld seam surfaces but large weld roots. In turn, high welding speeds and welding currents
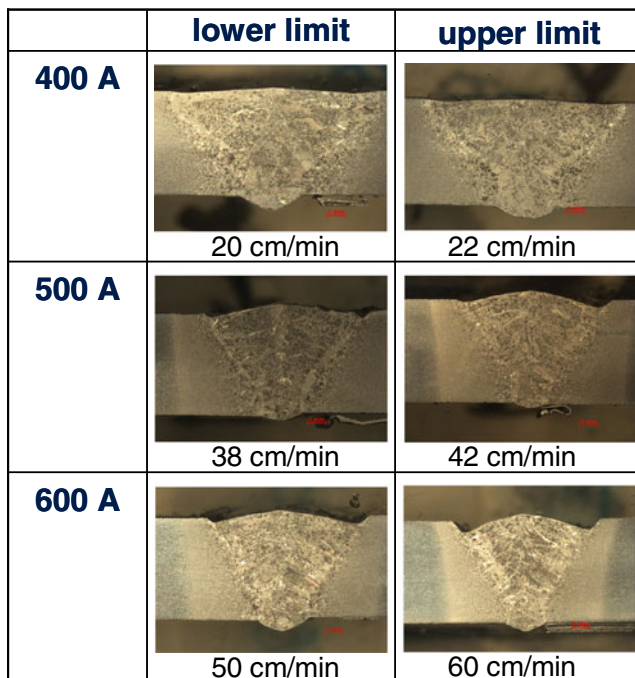

Fig. 15 Cross sections of CF-TIG-welded 6-mm-thick mild steel specimens with a CWD of 0.5 mm

induce a more V-shaped fusion zone and undercut. Considering the cross sections from Fig. 15, no weld imperfections can be found.

4.2 Mild steel plates up to 12 mm

After being able to realize good welding results for 6-mm-thick mild steel metal plates, the CF-TIG process was briefly tested for thicker specimens. The welding current was set to 600 A and the CWD to 0.5 mm. The welding speed was lowered for thicker test specimens. The resulting cross sections of the tests are shown in Fig. 16. From the pictures, it can be concluded that mild steel up to 11 mm in thickness can be welded. Again, undercut and underfill cannot be prevented. The first results for 12-mm-thick metal plates show lack of fusion. The weld root formation is insufficient as well, since the plate edges are not properly melted into the weld seam root. However, it can be argued that the welding current of 600 A is too low for metal plates that thick.

5 Summary

Due to extensive test series, it could be shown that the CF-TIG process works well for stainless and mild steels in the range of 6 to 10 mm in thickness and welding currents from 400 to 800 A. Very high welding speeds are possible, but the issue of undercut and underfill has to be investigated further. In turn, very good seam qualities can be achieved for low welding speeds. Furthermore, a very good gap bridging ability could be shown, pointing out that the process handles tolerances very well. The wide possible range for the distance between cathode tip and work piece surface underlines this assumption.

If the CF-TIG process is to be used solely for joining thick metal plates, the risk of undercut and underfill has to be considered, e.g. by adding a trailing GTA process for smoothing the surface and/or to add filler material. This trailing process could also be extended by oscillating magnetic arc deflection.

Furthermore, the applicability of the process to weld the root faces of Y- and double V-groove weld preparations should be investigated. In these cases, the partially appearing undercuts are to some extent tolerable, since the following
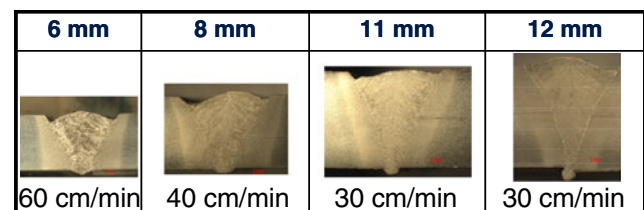

Fig. 16 Cross sections of CF-TIG-welded 6- to 12-mm-thick mild steel specimens with a welding current of 600 A and a CWD of 0.5 mm

welding process for filling the weld preparation will take care of it.

References

1. Jeffus L (2012) Welding: principles and application. Cengage Learning, Stamford
2. Grünenwald LS, Seefeld T, Vollertsen F, Kocak M (2010) Solutions for joining pipe steels using laser-GMA-hybrid welding processes. Physics Procedia 5:77–87
3. Ion JC (2005) Laser processing of engineering materials: principles, procedure and industrial application. Elsevier Butterworth-Heinemann, Oxford
4. Schnick M (2010) Numerische und experimentelle Verfahrens- und Brennerentwicklung beim Plasmalichtbogenschweißen. Diss., TU Dresden
5. Schnick M, Hertel M et al (2010) Plasma keyhole welding of mild steel plates for ship yard productions. 63rd International Conference of the International Institute of Welding, Istanbul, 2010. Document number: CONF-2010-AWST-10 57
6. Lancaster JF (1984) The physics of welding. International Institute of Welding, Pergamon Press, London
7. Demars P (1967) Le Soudage Plasma. Soudage et techniques connexes 22(5):181–202
8. Rosellini C, Jarvis L (2009) The keyhole TIG welding process: a valid alternative for valuable metal joints. Welding International 5(8):616–621. doi:10.1080/09507110802543237, http://www.tandfonline.com/doi/abs/
9. http://www.ultratig.com/. Accessed 12 April 2011, now http://www.k-tig.com/.
10. JE Fuentes, J Zschetzsche, M Schnick, U Füssel (2009) DE102007031534A1. Patent 2009, EP 2 008 750 A1.
11. Schnick M, Fuentes JE, Zschetzsche J, Füssel U, Schuster H, Krink V, Huebner M, Szczesny M (2010) Cathode focussed TIG—fundamentals and applications. 63rd International Conference of the International Institute of Welding, Istanbul, 2010. Document number XII-1985-10
12. Fischer P, Kree V, Wiese G, Letzig D (1994) (GKSS-Forschungszentrum Geesthacht GmbH, Geesthacht). Ätzen von Schwarz-Weiß-Verbindungen. In German. http://www.dgm.de/download/tg/686/686_36.pdf. Accessed 25 June 2013